Preprints of the 21st IFAC World Congress (Virtual)
Berlin, Germany, July 12-17, 2020

Predictive In-Cycle Closed-Loop Combustion Control with Pilot-Main Injections

Jorques Moreno, Carlos * Stenlåås, Ola * Tunestål, Per **

* *Scania CV AB, Södertälje, Sweden (e-mail: carlos.jorques@scania.com, ola.stenlaas@scania.com)*
** *Department of Energy Sciences, Lund University, Lund, Sweden (e-mail: per.tunestal@energy.lth.se)*

Abstract: This paper studies the use of predictive in-cycle close-loop combustion control to reduce the stochastic cyclic variations of diesel combustion. The combustion metrics that fully define the pressure trace with a pilot-main injection i.e. pilot and main start of combustion, burned pilot mass, and engine load are used as the set-point reference. These metrics are in-cycle predicted by calibrated models as functions of the current cylinder state, estimated by in-cylinder pressure measurements. The proposed approach uses four individual controllers for the set-point error minimization, which respectively regulate the injection's timing and duration of the pilot-main injection. The controllers are implemented in a FPGA and tested in a Scania D13 engine. The steady-state error reduction, disturbance rejection and transient response are discussed. The results confirm the error reduction in both, cycle-to-cycle and cylinder-to-cylinder variations. The error dispersion, measured by the 95% confidence interval, was reduced between 25% and 75% for all the controlled parameters. By on-line adaptation, the controllers are robust against model uncertainties and fuel types.

Keywords: Predictive control, diesel combustion, in-cycle closed-loop combustion control, pilot-main injection

1. INTRODUCTION

The combustion engine's combination of high reliability, robustness, high efficiency and energy density still makes them competitive against other alternatives. However, further reductions in their environmental impact, driven by the increasingly stringent emissions legislations, is required. This can be achieved by the further optimization of the engine operation, the development of advanced combustion concepts together with energy recovery systems, Willems (2018), and the use of sustainable fuels, Quirin et al. (2004). To tackle the additional complexity of these systems, closed-loop engine operation ensures their combustion stability and safety, and the increase in the performance robustness, Willems (2018). Closed-loop operation can inherently compensate for operational variations due to production tolerances, ageing, and external factors such as humidity or temperature of the intake air, Hui Xie et al. (2011). Furthermore, this increases the flexibility of the engine to use alternative fuels, such as biofuels, to adapt its operation to their different chemical properties. The required calibration is also reduced. Time consuming feed-forward map-based calibration of the operating variables is replaced by the set-point optimization, accomplished independently of the operating conditions by feedback algorithms.

The combustion process itself has a significant impact on the energy efficiency and emissions formation. In heavy-duty diesel engines, pilot fuel injections are used to reduce the main injection's ignition delay. This reduces the combustion rate, allowing a combustion timing closer to the maximum torque efficiency while fulfilling the noise and emissions constraints. The injected pilot mass is minimized while assuring its auto-ignition. However, injectors are designed for long main injections dimensioned at the peak torque. This results in high uncertainty for short pilot injections, which have a significant impact on the pilot's combustion, Jorques Moreno et al. (2017b) and effect on the main combustion, Jorques Moreno et al. (2017a). Therefore, high tolerances for the nominal pilot mass are necessary. To further reduce the pilot mass quantity under these uncertainties, this paper focuses on the minimization of the stochastic variations of the pilot combustion and its effects on the main injection's combustion.

The most common approach to control the combustion is by cycle-to-cycle control of the injection pulses, which is able to reduce the deterministic part of the variations and improve the cylinder balancing, Willems (2018). However, this does not suppress the stochastic cyclic variations that are the main source of the pilot combustion's variations, Jorques Moreno et al. (2017b). Therefore, in-cycle control of the combustion has great potential to overcome these limitations. In-cycle closed-loop combustion control is not as extended in the literature as cycle-to-cycle control. In the lack of other suggested methods, this article uses methods previously developed by the authors. Nevertheless, in-cycle control has been used previously for the reduction of the stochastic variations of the accumulated heat release,

Zander et al. (2010), NOx formation, Muric et al. (2013) and pressure trace evolution, Steffen and Yang (2012).

In Jorques Moreno et al. (2018a), the controller adjusted the main injection to maximize the indicated thermal efficiency under pilot combustion uncertainties. The equations were linearized at the nominal pilot mass to derive an explicit controller. The linearization proved to be a limiting factor to fully compensate for high pilot disturbances, specially significant for pilot misfire. This article investigates how to overcome the previous controller limitations, with a different approach. The stochastic variations around relevant combustion parameters, used as the set-point reference, are minimized. The reduction of the variations implies an engine operation closer to the optimal and the allowance of lower tolerances on the set-point, both with a net effect of a higher average engine efficiency.

This investigation extends the work presented in Yang et al. (2014) and Zheng et al. (2009). In the first one, the main injection was regulated to compensate for EGR variations, where feed-back was obtained from the pilot SOC. In the second one, the combustion phasing and load were regulated by the adjustment of a post injection, which compensated for disturbances in the main injection. In the present paper, predictive models are used to account for the variations of the intake conditions, pressure trace evolution and combustion rate of the multiple injections. The results discuss the reduction in the stochastic variations of the regulated variables at steady-state conditions, disturbance rejection, transient operation and robustness against different fuel types.

2. CONTROLLER DESIGN

2.1 Control targets

The stochastic variations of the combustion are a consequence of fluctuations in the inlet conditions (pressure, temperature and gas composition), the fuelling (rail pressure and injection rate), the combustion thermo-chemistry process (ignition delay and combustion rate), and the thermodynamic evolution, affected by the heat transfer. The in-cycle controller adjusts the fuel injection to compensate for these variations around the reference. The set-point reference may be calibrated off-line or adjusted on-line. A controller may determine the optimal adjustment of the set-point to account for the deterministic variations on a cylinder-to-cylinder and cycle-to-cycle context. It is out of the scope of this investigation how the set-point is determined.

2.2 Controller feedback

The inherent delay between the control action (fuel injection) and the system output (combustion) requires a predictive structure for the in-cycle adjustment of the injection. The controlled parameters have to be predicted from the current available measurements. The reference combustion metrics are selected to fully define the pressure trace. With a pilot-main injection, these are the pilot start of combustion, the burned pilot mass, the main start of combustion and the engine load. Each of these parameters are directly controlled with the injection timings and durations.

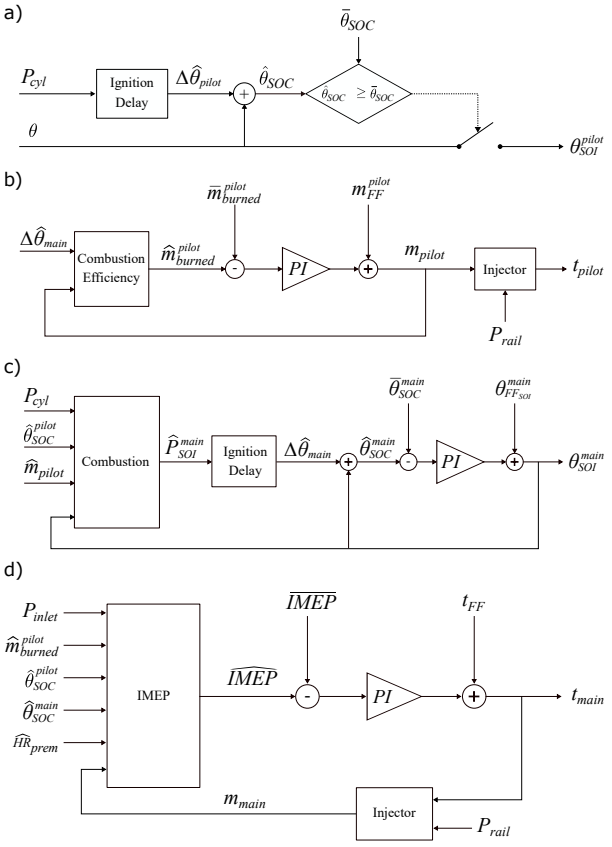

Fig. 1. Pilot SOI controller (a), pilot mass controller (b), main SOI controller (c) and main mass controller (d). P_{cyl} - Cylinder pressure, P_{rail} - rail pressure, θ - CAD, $\Delta\theta$ - ignition delay, θ_{SOI} - SOI, θ_{SOC} - SOC, m - fuel mass, t - injection duration, $IMEP$ - engine load, HR_{prem} - premixed heat release. Hat represents estimated value and bar the set-point.

2.3 Controller structure

There are four controllers. Each of them considers one of the individual control actions, following the temporal sequence. Their structure is illustrated in Fig.1.

Pilot SOI control. The controller uses the pilot SOC prediction (θ_{SOC}) by the ignition delay model ($\Delta\hat{\theta}$) to determine if the pilot SOI must be advanced to match the reference ($\bar{\theta}_{SOC}$). To ensure the stability of the controller, the ignition delay prediction is saturated to avoid an early SOI command.

Pilot mass control. The pilot combustion efficiency is predicted as a function of the in-cylinder thermodynamic conditions, which includes the effect of the controlled SOI. The controller is a PI regulator that iterates to converge to the reference. The commanded duration is computed with the injector's model, see Subsection 3.5.

Main SOI control. The main combustion timing control uses the same approach as the pilot SOI controller. The

effect of the pilot combustion must be included in the main ignition delay prediction. In the model, the pilot mass burned is used. It can be estimated in-cycle with e.g. the proposed method in Jorques Moreno et al. (2018a) or future developed methods. When no direct measurements are available before the pilot SOC, it is predicted together with the main SOC. Based on this prediction, the main SOI is adjusted by a PI controller to converge to its SOC reference.

Main mass control. A PI regulator is selected to minimize the error between the IMEP prediction and the reference. The injection duration is regulated instead of the mass to avoid division of the injector's model (section 3.5, Eq.7). Direct feedback from the main combustion heat release can be obtained for long injections i.e. the injection ends after the SOC ($\theta_{SOC} < \theta_{EOI}$). The main SOC and premixed heat release peak (HR_{prem}) are the measurements used to update the IMEP prediction.

3. PREDICTIVE MODELS

The predictive models overcome the lack of direct measurements of the controlled variables while there is still controllability within the same cycle. The controllers' performance is directly related to the prediction accuracy. Highly accurate models will require of highly complex expressions, which is limited by their real-time implementation. Instead, simple models that can capture the influence of the measured disturbances are used. The models are adapted on-line individually for each cylinder to improve their accuracy while maintaining a reduced complexity. They are briefly described in this section.

3.1 Ignition delay

Pilot ignition delay. Different models can be used, such as the suggested in Finesso and Spessa (2014) or Jorques Moreno et al. (2018b). The latter is used in this investigation:

$$\Delta\theta_{pilot} = Ke^{\alpha P_{SOI}} + \beta P_{rail} + \Delta\theta_0 \tag{1}$$

Main ignition delay. A simple model that can be computed in a single step was chosen. It is hence limited to a certain range of operating conditions. The model has to be accurate in a limited range, where the measured disturbances, i.e. pilot combustion, and control variable, i.e. main SOI, vary:

$$\Delta\theta_{main} = Ke^{\alpha P_{SOI}} + \beta(m^{pilot}_{burned} - m_0)^2 + \Delta\theta_0 \tag{2}$$

3.2 In-cylinder pressure

It is modelled as a polytropic process, i.e. $PV^{\kappa} = C$. The volume is estimated from the position of the crank-shaft, including possible deviations due to high in-cylinder pressures, West et al. (2018). The constant C is estimated at a given reference CAD position and measured pressure. The polytropic coefficient κ is estimated within the cycle, explained in section 4.

3.3 Pilot combustion

It is modelled as an isochoric combustion:

$$\Delta P = \frac{\kappa - 1}{V}(m_{pilot}\eta_{comb}Q_{LHV}) \tag{3}$$

The combustion efficiency is predicted by the experimental model suggested in Jorques Moreno et al. (2018a):

$$\eta_{comb} = \frac{a - b(\Delta\theta_{pilot} - \theta_0)}{1 + e^c(m_{pilot} - m_0)} \tag{4}$$

The model is calibrated to minimize the error in the pressure increase (Eq.3).

3.4 IMEP

The IMEP prediction is done by an empirical model which uses the measured and commanded in-cycle variables as inputs i.e. the inlet pressure, the pilot mass, the main combustion timing, the main mass and the main heat release premixed peak:

$$\begin{aligned} IMEP = k_0 m_{main} + k_1\theta^{main}_{SOC} + k_2 P_{IVC} + \\ k_3 m_{pilot} + k_4 HR_{premixed} + k_5 \end{aligned} \tag{5}$$

Some of the variables used may not be measurable during the time window when control action is possible. The predicted values are used instead in those scenarios.

Premixed heat release peak. It is modelled as a function of the main ignition delay and the burned pilot mass:

$$\begin{aligned} HR_{premixed} = a + b\Delta\theta_{main} + c\Delta\theta_{main}m^{pilot}_{burned} + \\ d(m^{pilot}_{burned} - m_0)^2 \end{aligned} \tag{6}$$

3.5 Injectors

For short pilot injections, a third order polynomial models the on-time with the fuel mass and the rail pressure as independent variables. For the main injection, the fuel mass is modelled by Eq.7:

$$m_{inj} = a + b \cdot t_{inj} \cdot (P_{rail} + c) \tag{7}$$

4. VIRTUAL SENSORS

The main sensors used for the monitoring of the combustion are the crank-shaft position, the in-cylinder pressure, rail pressure, inlet manifold pressure and temperature. Virtual sensors are required to estimate the variables not measured directly used for the predictions.

For the in-cycle pilot mass estimation, a simplified version of the method proposed in Jorques Moreno et al. (2018a) was implemented. Only the heat release magnitude, with a $\pm 0.5mg$ accuracy, was used.

Different methods to determine the polytropic coefficient can be found in the literature, such as the NASA polynomials or in-cycle instantaneous estimation methods, Zander et al. (2010). To avoid the computational complexity

of the first and the sensitivity to measurement noise of the second, an equivalent constant polytropic coefficient was used. This requires the assumption of a constant heat capacity ratio, and the ideal gas behaviour of the bulk mass inside the combustion chamber, which is valid under a limited CAD interval. Using recursive least squares, the polytropic coefficient is estimated to minimize the pressure prediction error. Taking logarithms on the polytropic compression:

$$\log P(\theta) = \kappa(\log(V_0) - \log(V(\theta)) + \log(P_0) \quad (8)$$

The prediction step on $\log(P(\theta_i)) = Y_i$ is:

$$\hat{Y}_i = \hat{\kappa}_{i-1}(\log(V_0) - \log(V(\theta)) \quad (9)$$

For the correction step, the update factor α is calibrated as a trade-off between convergence speed and the final error accuracy:

$$\hat{\kappa}_i = \alpha(Y_i - \hat{Y}_i) \quad (10)$$

The initial point for the estimation must be calibrated so that the assumptions hold. A good trade-off between an early reference point while having a low variation of the polytropic coefficient was found at $-40CAD$. An accurate initial estimation of the polytropic coefficient will also minimize the pressure prediction error.

5. MODEL ADAPTATION

The models were adapted to improve their prediction accuracy. The adaptation improves the controller robustness against dynamics not captured by the models, cylinder-to-cylinder variations, tolerances and ageing of the components. For the adaptation, simple methods are used, aiming to illustrate how the performance of the in-cycle controller can be improved. For the linear in parameters models, recursive least squares methods were used. For the non-linear models, a non-linear least squares criterion was applied with a gradient descent method. The model adaptation is done in a cycle-to-cycle basis and individually for each cylinder. The implementation is outside the FPGA, where additional computational resources and time are available.

6. EXPERIMENTAL SETUP

The in-cycle CLCC was tested in a modified Scania D13 Heavy-Duty engine. The XPI injection system was used for the multiple injections. The controller was implemented in three levels. The fast in-cycle control was implemented in a NI PXI-7854/7854 R (Multifunction reconfigurable I/O with Virtex 5-LX110/LX30 FPGA). The real-time controller was implemented in a PXI chassis (NI PXIe-8135 2.3 GHz quad-core processor) and executed at 100Hz. The user interface was implemented in LabView on a Windows 7 PC, which used the TCP/IP protocol for communication. More details of the experimental setup can be found in Jorques Moreno et al. (2017b).

7. RESULTS AND DISCUSSION

7.1 Steady-state controller performance

Set-point error. The results of the measured dispersion of the controlled variables, over 100 combustion cycles, at different steady-state reference points, are summarized in Fig. 2. The controller achieves an overall accurate reference tracking.

The in-cycle control of the pilot SOC (top-left plot in Fig.2) is mostly effective for early SOC references, where the intake conditions have a more significant effect on the pilot's combustion variability. The error is reduced from $\pm 1CAD$ to $\pm 0.4CAD$. For later SOC, the pilot combustion is more stable and the in-cycle control does not improve the performance significantly. The main SOC dispersion can also be reduced, see lower-left plot in Fig.2. The reduction is mostly due to decreased cylinder-to-cylinder variations. The cycle-to-cycle dispersion was reduced for the cases of small pilot masses and low loads, where the pilot combustion's effect is more significant than the random variations, which could not be reduced further than $\pm 0.3CAD$. This resulted in a similar cycle-to-cycle dispersion for open-loop and closed-loop operation when the combustion of the pilot was stable. The error of the pilot burned mass (top-right plot in Fig.2) can be reduced from $\pm 1.5mg$ to $\pm 0.6mg$. For small pilot masses, the controller can reduce the risk of misfire, see the case of $2mg$. For early pilot SOC ($-16CAD$), there is an off-set error due to the limitation of the combustion efficiency. However, the controller is able to reduce the error. Similar trends are obtained for the different engine loads (lower-right plot in Fig.2). The error is reduced from $\pm 0.8bar$ to $\pm 0.2bar$ IMEP. By the use of the in-cycle controller, the indicated efficiency was improved from 20% to 28% at $2bar$ IMEP due to the higher pilot combustion robustness and the main ignition delay adjustment when using the controller. At low loads, the efficiency was increased from 26.5% to 29.0%. As the load increases, the variations are less significant, reducing the efficiency improvement to $+0.37\%$ units.

Disturbance rejection. The cross-coupling of the multivariate system may alter the set-point error at different operating conditions. The models use a number of variables for the prediction, which alleviates the cross-influence between them, and in general the effect on the error performance is minimal. However, there are some cases that require special attention.

The first is how the pilot combustion is affected by the engine load. The engine load sets the intake conditions and the engine temperature, which have a significant effect on the pilot combustion, Jorques Moreno et al. (2017b). The mass burned of the pilot as a function of the engine load is plotted in Fig.3. There are two distinguished regions. At low loads, the lower engine temperature is not sufficient to trigger the pilot combustion in open-loop operation. The in-cycle CLCC can compensate for it for some of the cycles, increasing the average burned pilot mass from $0mg$ to $3mg$. As the load increases, the misfire events can be fully compensated (see the case at $4bar$ IMEP). In open-loop operation, the total dispersion ($\pm 1.5mg$) is

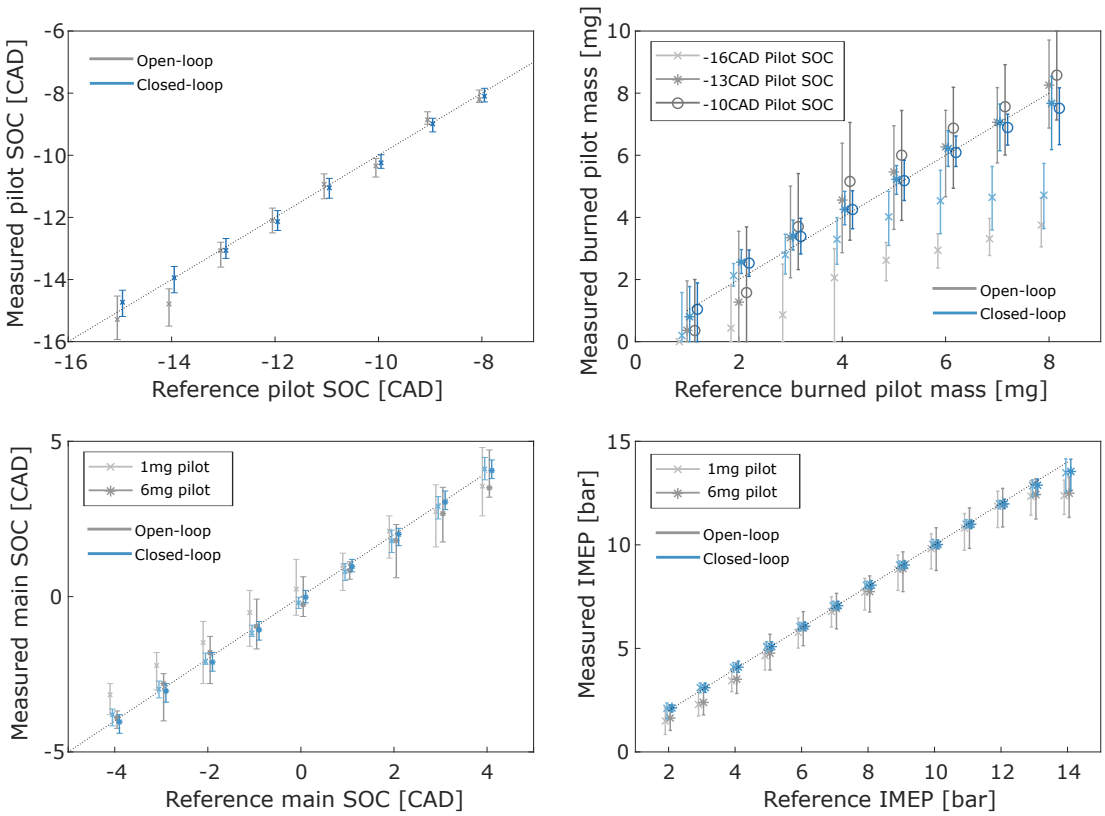

Fig. 2. Steady-state results at $1200RPM$, $1200bar$ rail pressure. Different pilot set-points are used around the nominal, set at $10bar$ IMEP, $6mg$ burned pilot mass and $-13CAD$ pilot SOC. The bars are the 95% confidence interval.

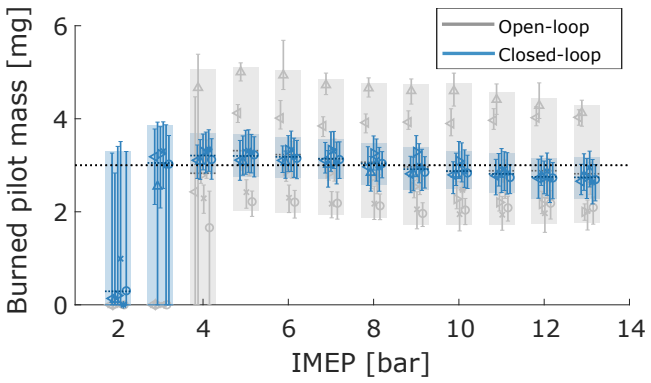

Fig. 3. Steady-state burned pilot mass at $-13CAD$ SOC for different engine loads, at $1200RPM$, $1200bar$ rail pressure. The bars are the 95% confidence interval.

mainly due to cylinder-to-cylinder variations ($\pm 0.5mg$). For closed-loop operation, the dispersion is reduced around the reference and similar for all the cylinders, with an error of $\pm 0.6mg$. For medium-high loads, the cycle-to-cycle dispersion is similar to open-loop operation, as the random variations cannot be reduced further. The indicated efficiency was improved from 26.9% to 28.12% at low loads by the reduction of the pilot disturbances. With the additional robustness of the pilot combustion at low loads, the nominal pilot mass can be reduced for a further improvement of the efficiency compared to open-loop operation. At higher loads, the efficiency improvement was limited to +0.4% units due to the lower sensitivity.

The second interesting variable is the main SOC as a function of the burned pilot mass, plot in Fig.4. For small burned pilot masses ($1mg$), the misfire events are not fully compensated. Despite the average error is reduced (from $1.7CAD$ to $1CAD$), there is still a high cycle-to-cycle dispersion ($\pm 0.6CAD$). At $2mg$ burned pilot mass, the in-cycle controller can achieve a more robust pilot combustion, reducing the error of the main SOC (from $0.7CAD$ to $0.3CAD$) and the cycle-to-cycle dispersion (from $\pm 1.2CAD$ to $\pm 0.3CAD$). For higher burned pilot masses, the error and dispersion is similar in open and closed-loop ($\pm 0.3CAD$), mostly reduced for early pilot injections, more sensitive to the intake conditions. The IMEP is also influenced by the burned pilot mass. In open-loop operation, if the main mass not explicitly compensated for different pilot injections, the error on the IMEP is proportional to the total injected mass. This is automatically compensated with the in-cycle regulator.

7.2 Controller robustness

External disturbance sensitivity. Two external disturbances were studied, the rail pressure and the engine speed. The effect of these disturbances was successfully compensated with the proposed controller. In the case of the burned pilot mass, its dispersion was positively correlated with the rail pressure, with a dispersion from $\pm 0.6mg$ at 600bar rail pressure to $\pm 1.2mg$ at 1500bar. This is due to the fact that at higher rail pressures, the on-time must be reduced to maintain the same fuel injected mass. Additionally to higher rail pressure oscillations, the uncertainty on the actual opening of the injector tip increases

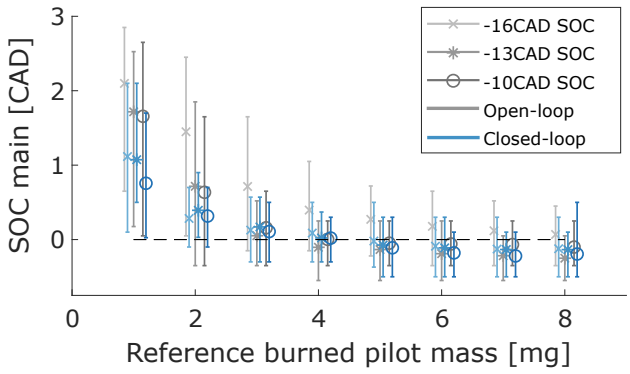

Fig. 4. Steady-state main SOC as function of the burned pilot mass at different pilot SOC, at 10*bar* IMEP, 1200RPM, 1200*bar* rail pressure. The bars are the 95% confidence interval

the variability of the injected mass. The dispersion of the pilot and main SOC were also slightly increased at low rail pressures, from $\pm 0.3CAD$ at 1200bar to $\pm 0.4mg$ at 600bar. This is due to the longer mixing time that increases the variations on the auto-ignition, Jorques Moreno et al. (2017b). Focusing on the engine speed, its influence on the burned pilot mass and engine load was compensated by the controller. However at higher engine speeds, the error dispersion of the pilot and main SOC were increased, from $\pm 0.3CAD$ at 1200RPM to $\pm 0.5CAD$ at 1400RPM, as a result of the higher turbulence, the increased pilot auto-ignition's stochasticity, increased signal noise and higher CAD resolution.

Model uncertainty sensitivity. The previous experiments were run with the off-line calibrated predictive models for diesel and no on-line adaptation. Three fuels were tested: Swedish S10 diesel fuel, Rapeseed Methyl Esther (RME) and Hydrotreated Vegetable Oil (HVO). The steady-state results for an individual sweep of each of the controlled variables are plotted in Fig.5. The set-point error is directly related to the model accuracy. When the models are adapted, the controller performance is robust against fuel uncertainties. The previous discussion of the controller performance is still valid for the results using the other fuels. By the model adaptation, the error of the pilot burned mass was reduced from $\pm 1.2mg$ to $\pm 0.6mg$ on average. The pilot and main SOC error was reduced from $\pm 0.6CAD$ to $\pm 0.3CAD$. The average engine load error was reduced from $\pm 0.7bar$ to $\pm 0.15bar$. The indicated efficiency was improved on average $+0.2\%$ unit. This may not seem as a significant improvement, but it must be noted that the controller is designed to follow the reference. The most significant improvement in the efficiency is from the reduction of the tolerances added to handle the higher operational margins from the fuel and parameter uncertainties.

7.3 Transient response

Set-point tracking. For the set-point tracking transient response analysis, different step sizes on the reference were commanded. The transient results on the IMEP set-point tracking are plotted in Fig.6. The transient of the IMEP takes about 20 cycles until it converges. The transient duration and the overshoot is caused by the model adaptation of all the variables. In fact, the overshoots were not found when the models were not adapted. The load change affects the pilot SOC tracking, that requires some time ($\sim$40 cycles) to re-adjust the prediction, mostly when the load is reduced, which results in long ignition-delays more sensitive to the intake conditions. The effect of the load change on the pilot mass is minimal. However, for low loads, the pilot auto-ignition may not be triggered. An unexpected result is found for large positive load steps. The feed-forward may cause an advance on the pilot SOI, which due to the delay on the load reference tracking results in the pilot misfire. This increases the error on the load reference tracking that oscillates before reaching the reference, once the pilot SOI controller has compensated for the actual load. Similar effect is found for negative load steps, where the pilot SOC controller over-compensates the pilot SOI, increasing the transient duration. The transient response of the controller is not improved compared to a cycle-to-cycle controller. However, the steady-state results are still improved, as discussed previously. Furthermore, the in-cycle controller reduces the cylinder-to-cylinder variations notwithstanding, being the cycle-to-cycle variations over the transient the remaining challenge for the controller.

The set-point tracking transient of the pilot combustion is plotted in Fig.7. The upper plot shows the pilot mass step responses, with a minimal duration ($\sim$5 cycles). Negative steps result in undershoots during the adaptation of the injectors' model. This may cause pilot misfire. See the case for $1mg$ where only misfire is obtained. When the set-point is increased again to $7mg$, the lack of feedback for the adaptation results in a delay until some pilot combustion is finally triggered. The cylinder-to-cylinder variations are increased due to the controller saturation of the pilot duration. This can be compensated with the addition of an adequate feed-forward for the in-cycle controller. In the lower plot, the pilot SOC transient duration is plotted. For robustness reasons, the adaptation is longer ($\sim$30 cycles). The longest transient is found for early SOC references (see the case at $-15CAD$), which takes $\sim$50 cycles. The ignition-delay model is more sensitive and less accurate at this region, requiring a longer adaptation time. The effect of the pilot transients on the other controlled variables was less significant than the effect of the engine load.

The main SOC transient is plotted in Fig.8. The transient duration is minimal ($\sim$5 cycles), but there is an instability when the reference is set at $-5CAD$. From the adaptation of the previous set-point, the model predicts a long ignition-delay that sets the main SOI at an early CAD. The consequent short pilot-main separation results not only in the lack of direct feedback from the pilot combustion, but also in difficulties to fully close the injector between injections. The actual injected mass becomes disturbed and the controller becomes unstable due to the adaptation of the main ignition delay and load models. A minimum separation is therefore required in the controller.

Model adaptation. The most significant part of the transient duration was due to the adaptation of the predictive models. For its detailed study, the engine was run in closed-loop mode with the off-line calibration. Then, the adaptation was started. The IMEP adaptation converged after 5 cycles. The pilot mass required around 10 cycles. To reduce

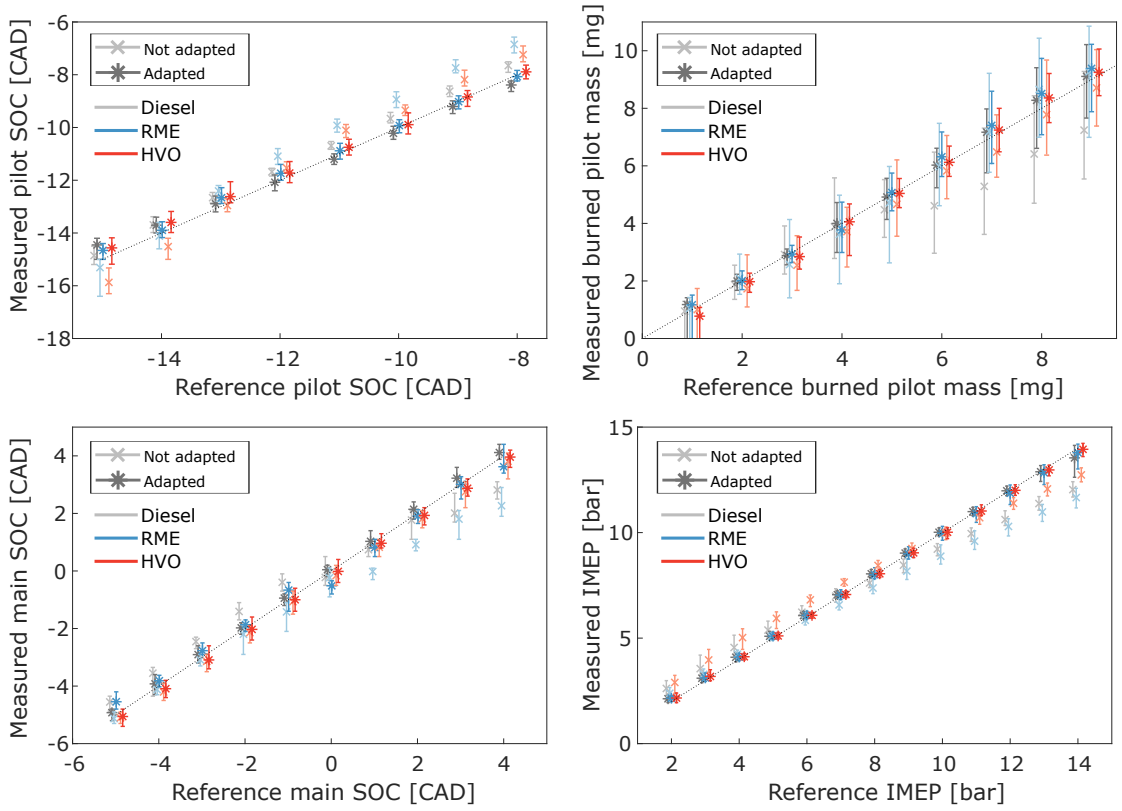

Fig. 5. Steady-state results with non-adapted and adapted in-cycle CLCC. Engine run at $1200RPM$, $1200bar$ rail pressure. Nominal load $10bar$ IMEP, $6mg$ burned pilot mass and $-13CAD$ pilot SOC. The bars are the 95% confidence interval.

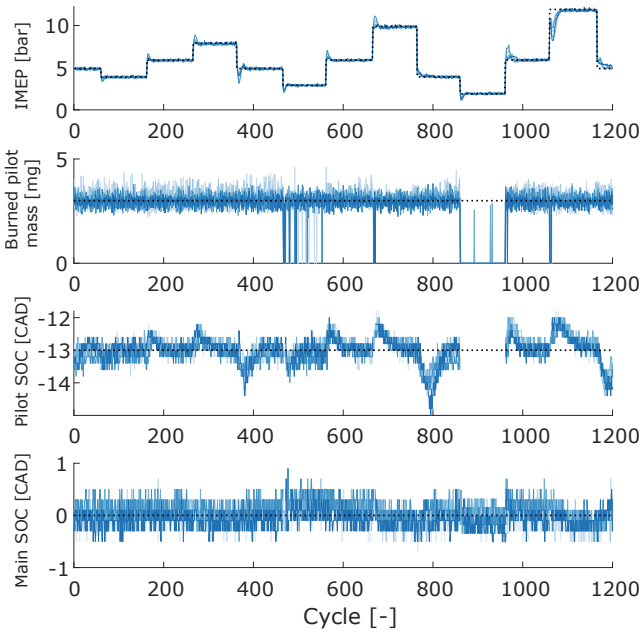

Fig. 6. IMEP set-point transient. Engine run at $1200RPM$, $1200bar$ rail pressure.

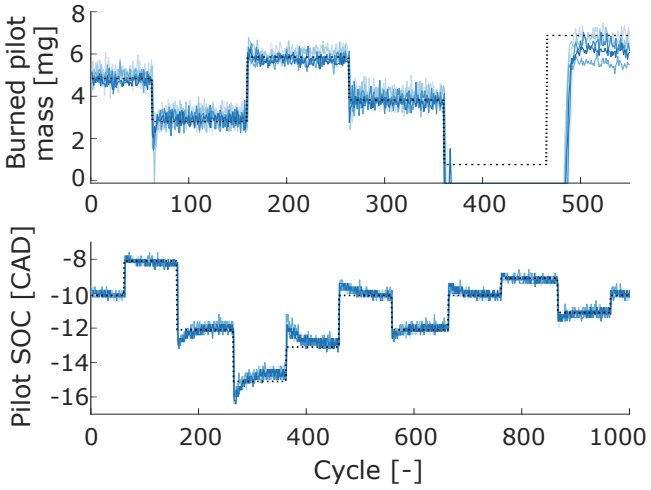

Fig. 7. Burned pilot mass and SOC set-point transient at $10bar$ IMEP, $1200RPM$, $1200bar$ rail pressure. Nominal pilot was set at $-13CAD$ SOC and $3mg$ burned fuel mass.

the influence of the measurement noise, the SOC adaptation was the slowest to converge, about 15 cycles were required. The adaptation rate must be considered for the tuning of the in-cycle controller as the cross-coupling of the controlled variables may increase the transient over-shoots and even destabilize the controller. Model adaptation has to be considered in the controller design. On one hand, to avoid instabilities saturation in the controlled outputs are required. On the other hand, to avoid long transients and oscillations, accurate models over a wider range of operating conditions can overcome the limitations of the proposed models. More advanced adaptation techniques will also help to reduce the transient response.

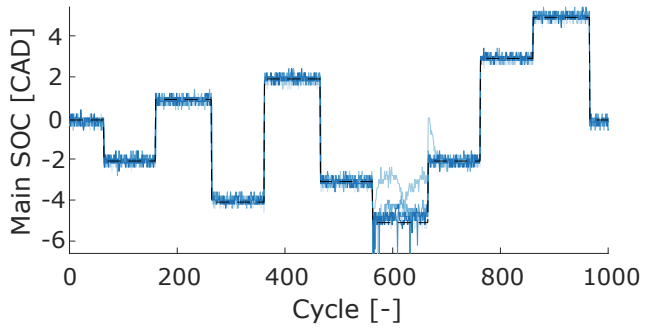

Fig. 8. Main SOC set-point transient, at 10bar IMEP, 1200RPM, 1200bar rail pressure. Pilot was set at $-13CAD$ SOC and 3mg burned fuel mass.

8. CONCLUSION

A predictive in-cycle closed-loop combustion controller is proposed in this study. The controller regulates the combustion with a pilot and a main injection. The reference is specified by four parameters: the pilot SOC, the burned pilot mass, the main SOC and the engine load (IMEP). Due to the ignition-delay of the combustion, the controller uses predictive models for the in-cycle regulation. Each parameter is controlled individually by a dedicated regulator. The cross-coupling effect of the variables is included in the predictive models.

A Scania D13 engine was used to perform the experiments. The set-point error and disturbance rejection in steady-state were analyzed. The analysis focused on the reduction of stochastic cyclic variations on a cycle-to-cycle and cylinder-to-cylinder basis. Measured by the 95% confidence interval, the variations were reduced from $\pm 1CAD$ in open-loop to $\pm 0.4CAD$ in closed-loop for the pilot SOC, from $\pm 1.5mg$ to $\pm 0.6mg$ for the burned pilot mass, from $\pm 0.4CAD$ to $\pm 0.3CAD$ for the main SOC, and from $\pm 0.8bar$ to $\pm 0.2bar$ IMEP for the engine load. The variations reduction is less significant at higher load as the combustion process becomes more robust.

The controller is specially effective at operating conditions with high sensitivity to the pilot combustion, such as high EGR rates and early pilot injections. Due to its predictive structure, the use of the in-cycle controller can reduce the dispersion of a cycle-to-cycle regulator in steady-state. The regulator performance is directly correlated to the model prediction error, which is minimized by online adaptation of the models. This allows the use of more computationally efficient models, with a reduced calibration effort, over a wide range of operating conditions and fuels. However, care must be taken when the models are adapted. The adaptation of the models affects the transient response and may lead to instabilities if the cross-coupling of the variables is not considered. Pilot misfire was not fully compensated with the proposed regulator. Models valid in a wider range of operating conditions and more advanced adaptation techniques are suggested to improve the transient response. The set-point reference was not optimized at each operating conditions or for each cylinder. Research on how this can help to optimize the engine performance in emissions and efficiency is suggested for future work.

ACKNOWLEDGEMENTS

The authors acknowledge the Swedish Energy Agency for funding this research project (Grant number 22485-4), the Competence Center for the Combustion Processes (KCFP) at Lund University, LTH and Scania CV AB for the test equipment facilities and support.

REFERENCES

Finesso, R. and Spessa, E. (2014). Ignition delay prediction of multiple injections in diesel engines. *Fuel*, 119, 170 – 190.

Hui Xie, Richard Stobart, Per Tunestål, Lars Eriksson, Yiqun Huang, and Patrick Leteinturier (2011). Future Engine Control Enabling Environment Friendly Vehicle. *SAE Techcnical Pap.*, (2011-01-0697).

Jorques Moreno, C., Stenlåås, O., and Tunestål, P. (2017a). Influence of small Pilot on Main Injection in a Heavy Duty Diesel Engine. *SAE Tech. Pap.*, (2017-01-0708).

Jorques Moreno, C., Stenlåås, O., and Tunestål, P. (2017b). Investigation of Small Pilot Combustion in a Heavy Duty Diesel Engine. *SAE Int. J. Engines*, (2017-01-0718).

Jorques Moreno, C., Stenlåås, O., and Tunestål, P. (2018a). Cylinder Pressure based Virtual Sensor for In-Cycle Pilot Mass Estimation. *SAE Tech. Pap.*, (2018-01-1163).

Jorques Moreno, C., Stenlåås, O., and Tunestål, P. (2018b). In-Cycle Closed-Loop Combustion Control with Pilot-Main Injections for Maximum Indicated Efficiency. *IFAC-PapersOnline*, 51, 92–98.

Muric, K., Stenlåås, O., Tunestål, P., and Johansson, B. (2013). A Study on In-Cycle Control of NOx Using Injection Strategy with a Fast Cylinder Pressure Based Emission Model as Feedback. *SAE Tech. Pap.*, (2013-01-2603).

Quirin, M., Grtner, S., Pehnt, M., and Reinhart, G. (2004). CO2 Mitigation through Biofuels in the Transport Sector. In *Main Report*. IFEU - Institut for Energy and Enviromental Research Heidelber.

Steffen, Thomas, S.R. and Yang, Z. (2012). Challenges and Potential of Intra-Cycle Combustion Control for Direct Injection Diesel Engines. *SAE Techcnical Paper*, (2012-01-1158).

West, I., Jorques Moreno, C., Stenlåås, O., Jönsson, O., and Fredrik, H. (2018). ICE Cylinder Volume Trace Deviation. *SAE JENG*, (0022).

Willems, F. (2018). Is Cylinder Pressure-Based Control Required to Meet Future HD Legislation? *IFAC-PapersOnline*, 51, 111–118.

Yang, F., Wang, J., Gao, G., and Ouyang, M. (2014). In-cycle diesel low temperature combustion control based on SOC detection. *Appl. Energy*.

Zander, C.G., Tunestal, P., Stenlåås, O., and Johansson, B. (2010). In-Cycle Closed Loop Control of the Fuel Injection on a 1-Cylinder Heavy Duty CI-Engine. ICEF2010–35100 405–414. ASME.

Zheng, M., Tan, Y., Reader, G.T., Asad, U., Han, X., and Wang, M. (2009). Prompt heat release analysis to improve diesel low temperature combustion. In *Powertrains, Fuels and Lubricants Meeting*. SAE International.